26th ABCM International Congress of Mechanical Engineering
November 22-26, 2021. Florianópolis, SC, Brazil

COB-2021-0358
EVALUATION OF SURROGATE MODELS FOR HYDRODYNAMIC FORCES IN JOURNAL BEARINGS

Iago Oliveira de Almeida
Gregory Bregion Daniel
School of Mechanical Engineering, University of Campinas (UNICAMP)
i265298@dac.unicamp.br
gbdaniel@fem.unicamp.br

Abstract. *The healthy functioning of rotating machines can be associated with the adequate performance of the bearings, due to the significative influence of this component on the rotor's behavior. In general, the analysis of the dynamic behavior of the lubricating film is performed solving the Reynolds equation by the finite volume method, which has a high computational cost. In this context, this work evaluates the application of surrogate models for hydrodynamic forces in journal bearings, to assure high accuracy and low computational cost in the analysis of rotating systems by finite element method. For that, different surrogate models are investigated in this work, such as linear interpolation, cubic interpolation, spline interpolation and artificial neural network. The results of the rotor orbit in the rotating system using the surrogate models are compared with the results obtained through the finite volume method. The simulations carried out in this work show that the cubic interpolation and spline interpolation have promising results, since they are capable of improving the accuracy with a lower computational cost. Therefore, the results obtained in this work bring scientific contributions related to alternative methods to model the hydrodynamic bearings, aiming to assure a low computational cost and enable its application in real time monitoring systems for rotating machinery.*
Keywords: *surrogate models, journal bearing, hydrodynamic forces, rotordynamics.*

1. INTRODUCTION

Rotating machines constitute a class of machines widely used in several sectors of the mechanical industry. Therefore, developing technologies to ensure the operation of these machines with greater reliability and efficiency is of great relevance and demand. A topic that has received great attention is the mathematical modeling, increasing the representativeness of each component that composes these rotating machines. One of the crucial components for the operation of the rotors is the hydrodynamic bearing, which provides high load capacity and low friction coefficient for the machines.

Unlike other types of bearings, hydrodynamic bearings form a coupling between the rotating and static parts through a lubricating film, increasing its efficiency due to the low coefficient of friction. In general, researches involving hydrodynamic bearings seek to computationally simulate the dynamic behavior of this component through mathematical models in order to evaluate its influence on the rotor's dynamic behavior. Due to their operating conditions, hydrodynamic bearings operate based on their geometry and rotor rotational speed, creating a pressure field that provides the hydrodynamic forces acting on the system (Pinkus and Lynn, 1956). The inclusion of the hydrodynamic forces in the rotating system's equation of motion allows to perform simulations more consistent of the real machine. Due to the importance of hydrodynamic bearings in rotors, the demand to develop mathematical models capable of representing the dynamic behavior of these components is evident (Ramos, 2019). However, the greater the model's complexity, the greater its computational cost. Thus, the inclusion of effects, such as cavitation and thermal variation on the lubricating fluid, entail a large computational cost, demanding a high simulation time to determine the hydrodynamic forces (Sicchieri, 2019). For this reason, there is a need to apply alternative models capable of representing the non-linear dynamic behavior of hydrodynamic forces in journal bearings (Kornaev *et al*., 2017). In general, surrogate model fits simple analytic functions to represent high-cost computational models. However, there are different surrogate models that may be suitable for this application, thus requiring a careful evaluation to identify the advantages and limitations of the most recommended methods (Simpson *et al*., 2001).

2. PROPOSAL

Within this context, this paper is dedicated towards the application and comparison of surrogate models for the modelling of the hydrodynamic forces in journal bearings, in order to ensure high accuracy and low computational cost in the analysis of rotating systems supported by hydrodynamic bearings. For this purpose, different surrogate models are

investigated, namely, linear interpolation, cubic interpolation, spline interpolation and Artificial Neural Network (ANN). The numerical analyses are performed based on the rotor dynamic response in the time domain. In this section, the solution of the hydrodynamic forces by Finite Volume Method (FVM) is presented, along with the modeling of the rotating system by Finite Element Method (FEM) and the theoretical background related to the surrogate models employed in this work. Finally, the geometric and operational characteristics of the simulated rotor is presented.

2.1 Numerical Model of Hydrodynamic Journal Bearings

Figure 1 illustrates a section of a bearing-shaft assembly. In this figure, XYZ represents the inertial referential located in the bearing center (O_m), O_E represents the shaft center, e the eccentricity (distance between the bearing and the shaft centers), φ the attitude angle (angle between the center line and the vertical axis), Ω the rotational speed of the shaft, R the shaft radius, c_r the radial clearance and L the bearing axial length (width).

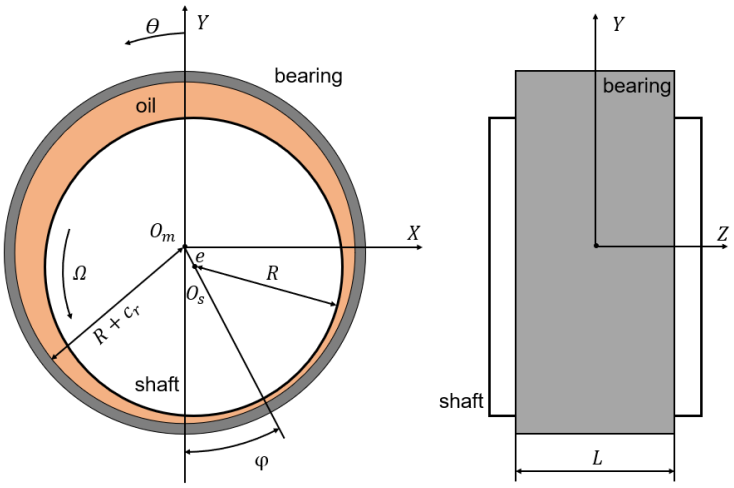

Figure 1. Section of a bearing-shaft assembly.

The mathematical representation of the lubricating fluid behavior inside the bearing is described by classical Reynolds equation, as presented in Eq. (1):

$$\frac{\partial}{\partial x}\left(h^3\frac{\partial P}{\partial x}\right)+\frac{\partial}{\partial z}\left(h^3\frac{\partial P}{\partial z}\right)=6\mu\Omega R\frac{\partial h}{\partial x}+12\mu\frac{\partial h}{\partial t}, \tag{1}$$

where μ indicates the dynamic viscosity of the lubricating fluid, h the film thickness, P the hydrodynamic pressure field and (x, z) the circumferential and axial coordinates, respectively. This mathematical model allows evaluating the pressure field along the bearing, making it possible to determine the acting hydrodynamic forces on the rotor.

In order to obtain the solution of the Reynolds equation by FVM, bearing's domain is divided in a finite number of control volumes, being N_x volumes of length Δx in the circumferential coordinate and N_z volumes of length Δz in the axial coordinate. The solution is obtained integrating the Eq. (1), considering the atmosphere pressure (ambient pressure) in the lateral border of the bearing and the circularity of the bearing domain as the contour condition. The solution of Reynold's equation by FVM for a generic volume P on the domain of the cylindrical bearing is presented as:

$$\left(h_e^3\frac{\Delta z}{\Delta x}\right)P_E+\left(h_w^3\frac{\Delta z}{\Delta x}\right)P_W+\left(h_n^3\frac{\Delta x}{\Delta z}\right)P_N+\left(h_s^3\frac{\Delta x}{\Delta z}\right)P_S-6\mu\Omega R\Delta z(h_e-h_w)$$
$$-12\mu\left(\dot{e_x}\sin\theta-\dot{e_y}\cos\theta\right)\Delta x\Delta z=P_P\left(h_e^3\frac{\Delta z}{\Delta x}+h_w^3\frac{\Delta z}{\Delta x}+h_n^3\frac{\Delta x}{\Delta z}+h_s^3\frac{\Delta x}{\Delta z}\right), \tag{2}$$

where the subscripts w, e, s, n indicate the west, east, south and north borders, respectively, the subscripts W, E, S, N indicate the west, east, south and north neighbors volumes, respectively, $\dot{e}_X$ and $\dot{e}_Y$ are the translational velocities of the eccentricity in the X and Y directions.

The convergence of the pressure field on the bearing domain is performed iteratively using the Gauss-Seidel method. The error between iterations is calculated by the total difference between the pressure fields of the current iteration and the previous iteration. After calculating the pressure field, the hydrodynamic forces acting on the journal bearing are calculated. Eq. (3) presents the hydrodynamic forces in the X and Y directions, based on the inertial reference of Figure 1,

$$F_X = \int_0^{2\pi R} \int_0^L P(x,z)\, sin\,\theta\, dz\, dx = \sum_{l=1}^{N_x} \sum_{k=1}^{N_z} P_{l,k}\, sin\,\theta_l\, \Delta x \Delta z,$$
$$F_Y = \int_0^{2\pi R} \int_0^L -P(x,z)\, cos\,\theta\, dz\, dx = \sum_{l=1}^{N_x} \sum_{k=1}^{N_z} -P_{l,k}\, cos\,\theta_l\, \Delta x \Delta z\,. \quad (3)$$

2.2 Numerical Model of Rotating System

In this work, the mathematical model of the rotor is developed by FEM, in which the rotors domain is discretized in continuous finite elements, as proposed by Nelson and McVaugh (1976). This model is composed of cylindrical Timoshenko beam elements and rigid disk element, in which each node has four Degrees of Freedom (DOF), being two translational displacements and two angular displacements (lateral vibration).

Using Lagrange equation, it is possible to obtain the system's equation of motion as described by Lalanne and Ferraris (1990),

$$[M_{global}]\{\ddot{q}\} + ([C_{global}] + \Omega[G_{global}])\{\dot{q}\} + [K_{global}]\{q\} = \{f_{global}\}, \quad (4)$$

where $\boldsymbol{M_{global}}$, $\boldsymbol{C_{global}}$, $\boldsymbol{G_{global}}$ e $\boldsymbol{K_{global}}$ are the mass, damping, gyroscopic and stiffness matrices, respectively, $\boldsymbol{f_{global}}$ is the vector of the external forces and $\boldsymbol{q}$, $\boldsymbol{\dot{q}}$, $\boldsymbol{\ddot{q}}$ are the displacement, velocity and acceleration vectors related to the inertial reference system. It is important to mention that the shaft damping matrix is calculated based on the proportional structural damping, as used by Tuckmantel (2010).

The global matrices are determined by the method of superposition of the matrices of the shaft and disc elements in their respective DOF. In this work, the external force applied to the rotor is composed of three main forces: weight force, hydrodynamic forces and unbalance forces. The weight force is constant and can be obtained from the mass of the rotor elements. Hydrodynamic forces have non-linear characteristics and vary as a function of the rotor's position and velocity and, consequently, as a function of time (Ramos, 2019). The unbalance force varies as a function of time and is calculated following the ISO 1940 standard, based on the balance quality grade (International Standard Organization, 2003). This force must be included in the vector of external forces in the respective DOF of the nodes that have unbalance. Once the global matrices and the external forces vector are determined, it is possible to obtain the displacement, the velocity and the acceleration of the rotating system in the time domain. This can be done through a numerical integrator. In this work, Newmark integrator was employed together with the Newton-Raphson search method, being one of the integrators commonly used in this type of analysis (Ramos, 2019).

2.3 Surrogate Models

Surrogate models are those whose parameters are adjusted to perform the regression or interpolation of data from an original model. They offer the greatest possible representation with a low computational cost. In this work, the surrogate models are employed in order to reduce the computational cost related to solution of the hydrodynamic forces, ensuring high accuracy in comparison with the FVM.

As previously stated, these models are based in a dataset from the original model and, in order to guarantee the model effectiveness, the dataset sampling must guarantee the representativeness of the proposed problem. According to Sacks *et al* (1989), a good sampling technique must fill the entire sampling space. One of the most used techniques that satisfies this approach is known as rectangular grid, which selects equally spaced values within the boundaries of the sampling space. Therefore, rectangular grid technique is employed in this work in order to obtain the database.

2.4 Artificial Neural Network (ANN)

According to Haykin (2009), an artificial neural network is a computational model massively distributed in parallel with simple processing units that have a natural ability to store knowledge and make it available for use. They are suitable for solving nonlinear problems with a high number of input variables due to their ability to change synaptic weights inside the neurons to adapt to the environment. One of the most employed neurons was proposed by Rosenblatt (1963), being known as perceptron. In summary, the neuron computes the output y_k through a linear combination of the input signals x_j, weighted by the synaptic weights w_{kj}, where k represents the neuron index and j indicates the input signal in which the weight is associated, and incorporates a bias b, generating then v_k, which passes through an activation function $\varphi_{at}(\cdot)$, usually of non-linear character, finally resulting in the output signal of the neuron y_k. Eq. (5) describes this relation between the input x_k and output y_k,

$$y_k = \varphi_{at}(v_k) = \varphi_{at}\left(\sum_{j=1}^{m} w_{kj}x_j + b\right). \quad (5)$$

When a set of neurons are combined and organized, they constitute an architecture. This architecture is defined by the type, the quantity and connectivity pattern established between each neuron. There are two main types of architecture, namely feedforward neural network (FNN) and recurrent neural network (RNN). One of the main exponents of the FNN architectures is the network known as the Multilayer Perceptron (MLP), that has the characteristic of an arbitrary number of hidden layers, also called hidden or intermediate layers, between the input and output of the network. The learning process of an MLP network is based on the optimization of synaptic weights and bias of all layers, in which the values that lead to the best input-output mapping for the network are searched. This optimization process is conducted iteratively, minimizing a cost function that describes an error between the outputs provided by the network and the desired outputs (Géron, 2019). One of the most employed cost functions is the Mean Squared Error (MSE), being used to train the networks in this work. Moreover, the cross-validation (CV) and the early stopping method is applied to train the neural network of this work, since it avoids common problems as underfitting and overfitting in the learning process by dividing the samples in two datasets: one to adjust the parameters (training dataset) and the other to monitor the model's generalization capacity (validation dataset) (Haykin, 2009).

2.5 Interpolation methods

Interpolation is a method to estimate the outputs of discrete functions at intermediate points based on a previously known set of data. The fundamental property of the interpolation functions is that they must match the sample data at the interpolation points, that is, whether $y(x_l)$ is a sampling point and $\hat{y}(x_l)$ is corresponding to the interpolation function, then $\hat{y}(x_l) = y(x_l)$, in which x_l are the interpolation points (Keys, 1981). Three types of interpolation functions are applied in this work, namely linear interpolation, cubic interpolation and spline interpolation.

The linear interpolation function can be interpreted as a weighted average of the nearest neighborhood to the desired output (Meijering, 2002). The cubic interpolation function is derived from a set of conditions imposed by an interpolation kernel within an interval, in which the approximation function is based on a third-degree polynomial (Keys, 1981). Lastly, spline interpolation function consists in the use of reduced degree polynomials in smaller sections of the total interval of the points, considering certain conditions that guarantee that the resulting approximation function is continuous and has continuous derivatives up to a certain order, avoiding the fluctuations caused by Runge's phenomenon (Lopes and Costa, 2017).

2.6 Description of the rotating system simulated in this work

In this work, the results were obtained considering a rotor-bearings system. The characteristics and operation conditions of the journal bearing are displayed in Table 1. Preliminary convergence tests were carried out in order to determine the proper size of the finite volume mesh, whose volumes numbers were $N_x = N_z = 40$, resulting a mean time of 50 ms to estimate the hydrodynamic forces. It is worth mentioning that the calculations related to this work were obtained from the software Matlab® in a personal computer with Intel® core™ i5-8265U CPU 1,6Ghz and 16GB RAM.

Table 1. Characteristics and operation conditions of the journal bearing.

Description	Symbol	Value	Unity
Diameter	D	31.0	mm
Width	L	20.0	mm
Dynamic viscosity	μ	50.0	mPa.s
Radial clearance	c_r	90.0	μm
Shaft rotation	Ω	15	Hz

Figure 2 presents the dimensions of the elements used on the rotor discretization. This rotor has a centralized disc and two journal bearings close to the ends. As illustrated in Figure 2, the model has 10 beam elements, a disc element and 2 bearing elements, being composed of 11 nodes and 44 DOF in total. Table 2 presents the characteristics of this rotor.

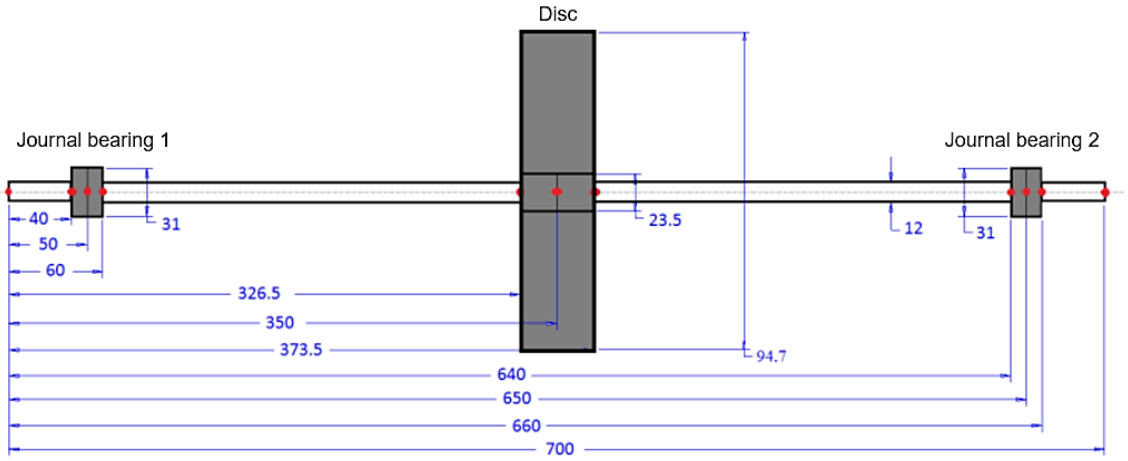

Figure 2. Finite elements rotor (units in millimeters).
Source: Ramos, 2019.

Table 2. Characteristics and operation conditions of the rotor.

Description	Symbol	Value	Unity
Modulus of elasticity	E	200.0	GPaGPa
Density	ρ	7850.0	Kg/m^3
Mass proportionality constant	α	0.0	1/m^{2}s
Stiffness proportionality constant	β	10^{-4}	s
Gravitational constant	g	9.81	m/s^2
1st critical frequency	–	22.5	Hz

3. RESULTS

Aiming to analyze the performance of the surrogate models for hydrodynamic forces of journal bearings, different databases were generated for training the ANN and interpolating the models. The databases were generated based on the solution of Reynolds equation by FVM. Four input features were considered in each surrogate model: the eccentricity ratio ($\varepsilon = e/c_r$), the attitude angle (φ) and the translational speeds of the eccentricity in the X and Y directions ($\dot{e}_X$ and $\dot{e}_Y$).

In order to determine the interval of each input feature, a time domain simulation of the rotor was performed. The total simulation time was 10 seconds. The rotor was unbalanced with the balance quality grade of 6.3 and the following initial conditions were set: accelerations and velocities of all DOF are considered null, the initial displacement is the static equilibrium position of the rotor supported by hydrodynamic bearings. Table 3 displays the limits obtained for the input feature domain.

Table 3. Journal bearing features.

Feature	Unity	Minimum	Maximum
ε	–	0.1	0.9
φ	rad	0	$\pi/2$
$\dot{e_X}$	m/s	-0.001	0.001
$\dot{e_Y}$	m/s	-0.001	0.001

The simulations performed in this work aims to apply the surrogate models considering a generic condition of the shaft inside the journal bearing, so the intervals for the features were selected seeking a wide range. Therefore, different databases were generated using the rectangular grid method, ranging from 4 to 10 samples per feature, as shown in Table 4. In all databases, the hydrodynamic forces F_X and F_Y were calculated by FVM given the known entries of the databases.

Table 4. Database characteristics for training/interpolation of surrogate models.

Number of samples per feature				Total number of samples into database
ε	φ	$\dot{e_X}$	$\dot{e_Y}$	
4	4	4	4	256
5	5	5	5	625
6	6	6	6	1296
7	7	7	7	2401
8	8	8	8	4096
9	9	9	9	6561
10	10	10	10	10000

The neural networks used in the work were generated and trained with the Matlab® software. In general, they are composed of an input layer with 4 neurons, three hidden layers with 10 neurons per layer, the activation function of neurons used in these layers is the logistic function, and an output layer with 2 neurons. The Levenberg-Marquardt method was used for training the ANNs, the databases were divided into two datasets, being 80% of the data destined for training and 20% for validation.

Linear, cubic and spline interpolation methods do not require a training step. The interpolations were performed using the functions of the Matlab® software, where the databases are provided and the output is calculated based on type of interpolation specified.

In this work, the surrogate models are applied in the solution of the hydrodynamic forces of the journal bearings to reduce computational cost. However, the evaluation of the surrogate models of journal bearings is performed simulating the rotor dynamic behavior, to ensure the best representation of these models based on the calculation made by the FVM. Figure 3 illustrates the extracted parameters of the rotor orbit inside the bearing in steady state, in which O_o represents the orbit center, e_{o-X} and e_{o-Y} are the distance of the orbit center with respect to the bearing center in the X and Y directions, respectively, R_{max} and R_{min} are the maximum and minimum radius of the orbit and, lastly, ψ_o is the inclination angle of the orbit.

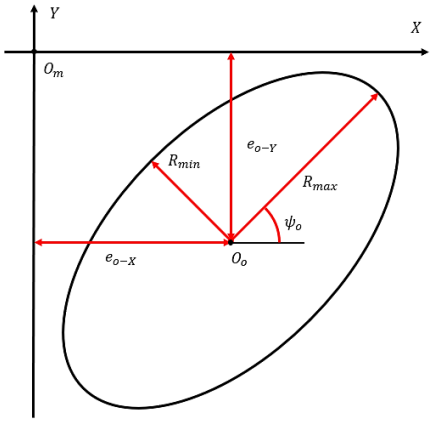

Figure 3. Schematic illustration of the parameters extracted from the rotor orbit.

In order to obtain the rotor orbits in steady state, computational simulations of the rotor's dynamic behavior were performed with the surrogate models of the journal bearings. In this work, the computational simulations of the rotor were performed during 10 seconds with a sampling frequency of 1 kHz and the steady-state condition was assumed only on the last second of the simulation (from 9 to 10 seconds). The rotor was unbalanced with the balance quality grade of 6.3.

Figure 4 presents the rotor orbits in steady state inside the journal bearings, i.e. the orbits of the nodes 3 and 9. In this figure, the blue orbit was obtained by FVM, the other orbits were obtained using ANNs with different number of samples and the black dotted line represents the bearing's radial clearance.

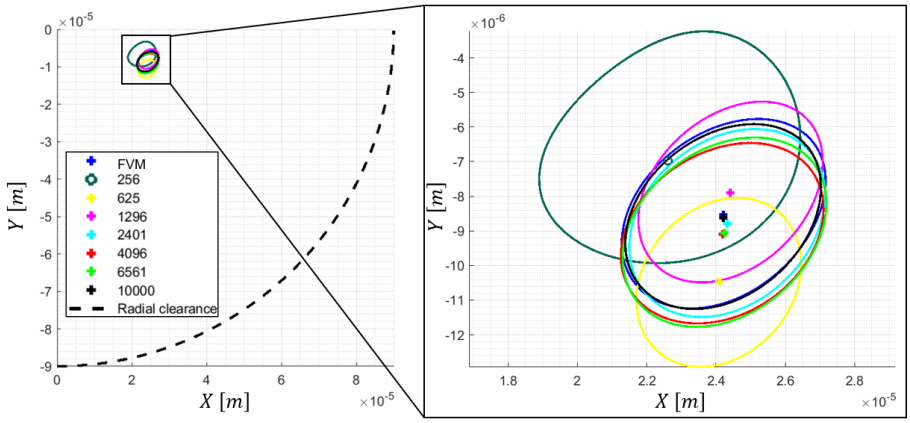

Figure 4. Comparison of rotor orbits in steady-state calculated by neural networks.

Table 5 presents the relative errors between the parameters obtained from the orbits calculated by FVM and by ANNs with different numbers of training samples, as shown in Figure 4. Moreover, the mean of the relative errors ($\boldsymbol{MRE_G}$) is also calculated in order to provide an overview of the behavior of the rotor orbit. Finally, the total time necessary to perform 10 seconds of simulation is presented (T_{sim}).

Table 5. Relative errors of the parameters obtained from rotor orbits calculated by ANNs using different numbers of samples for training.

Training samples database	**Assessment metric**						
	$\boldsymbol{RE_{e_{o-X}}}$[%]	$\boldsymbol{RE_{e_{o-Y}}}$[%]	$\boldsymbol{RE_{R_{min}}}$[%]	$\boldsymbol{RE_{R_{max}}}$[%]	$\boldsymbol{RE_{\psi_o}}$[%]	$\boldsymbol{MRE_G}$[%]	$\boldsymbol{T_{sim}}$ [s]
256	6.5793	18.1462	27.6442	24.4329	14.1458	18.1897	765.7336
625	0.4950	22.8742	7.5307	19.5442	20.2423	14.1373	793.2628
1296	0.8357	7.4330	6.0001	7.7827	9.9799	6.4063	778.8598
2401	0.4588	3.0947	1.4967	4.7195	6.0665	3.1672	781.0537
4096	0.1200	6.6288	1.6276	4.9769	7.8095	4.2325	771.3074
6561	0.1378	6.2469	2.9373	1.8605	1.7423	2.5850	771.7218
10000	0.0570	1.0135	1.2665	4.2955	4.8279	2.2921	752.5455

According to Table 5, it is possible to notice a significant improvement in the accuracy of the results for databases from 256 to 2401 training samples, while the accuracy improvement is practically stabilized for databases bigger than 2401 training samples.

The interpretation of Figure 5 and Table 6 are the same as those shown in Figure 4 and Table 5, differing only in the use of linear interpolation. The same can be said about Figure 6 and Table 7, that were obtained using cubic interpolation, and Figure 7 and Table 8, that were obtained using spline interpolation.

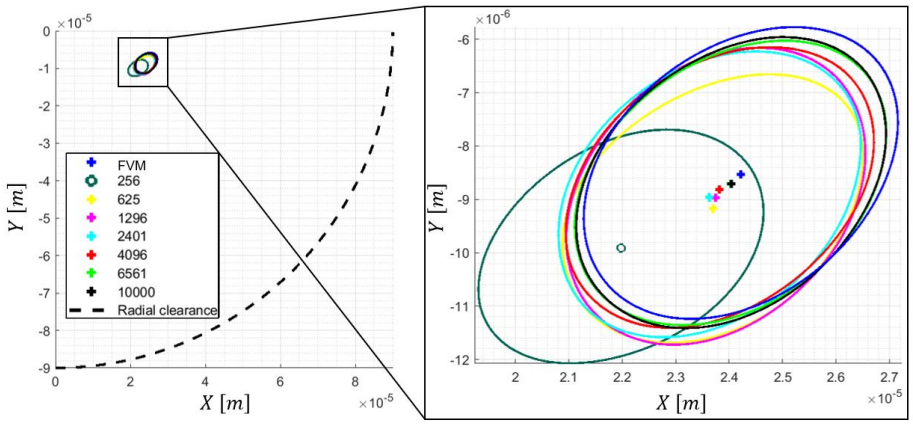

Figure 5. Comparison of rotor orbits in steady-state calculated by linear interpolation.

Table 6. Relative errors of the parameters obtained from rotor orbits calculated by linear interpolation using different numbers of samples.

Interpolation samples database	Assessment metric						
	$RE_{e_{o-X}}$[%]	$RE_{e_{o-Y}}$[%]	$RE_{R_{min}}$[%]	$RE_{R_{max}}$[%]	RE_{ψ_o}[%]	MRE_G[%]	T_{sim} [s]
256	9.2308	16.1603	16.7205	13.1836	18.1214	14.6833	93.6262
625	2.1104	7.4901	6.2671	4.8844	2.8524	4.7209	92.2671
1296	1.9345	5.0230	1.9916	4.0563	12.9649	5.1941	94.2157
2401	2.2990	4.9276	1.8342	3.3203	1.7503	2.8463	95.4649
4096	1.6300	3.3407	4.1370	2.8151	0.0141	2.3874	93.7373
6561	0.7657	2.0917	0.2669	1.6935	1.0741	1.1784	95.6268
10000	0.7245	2.0128	0.4423	1.5632	0.5006	1.0487	94.1831

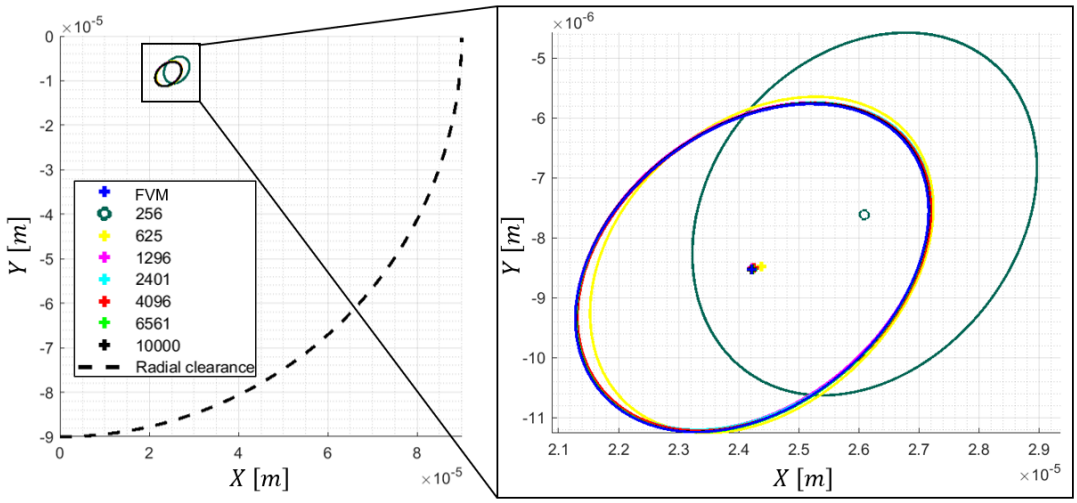

Figure 6. Comparison of rotor orbits in steady-state calculated by cubic interpolation.

Table 7. Relative errors of the parameters obtained from rotor orbits calculated by cubic interpolation using different numbers of samples.

Interpolation samples database	Assessment metric						
	$RE_{e_{o-X}}$[%]	$RE_{e_{o-Y}}$[%]	$RE_{R_{min}}$[%]	$RE_{R_{max}}$[%]	RE_{ψ_o}[%]	MRE_G[%]	T_{sim} [s]
256	7.7353	10.7477	10.5171	0.2708	25.3476	10.9237	108.2069
625	0.6521	0.6271	0.1110	1.0023	9.0778	2.2941	113.0364
1296	0.0341	0.2877	0.4580	0.3160	1.3291	0.4850	114.4098
2401	0.1373	0.3399	0.0753	0.4023	1.1387	0.4187	110.7188
4096	0.1572	0.2486	0.2582	0.0317	0.0545	0.1500	111.9166
6561	0.0426	0.0702	0.4387	0.0885	0.7046	0.2689	111.8045
10000	0.0173	0.0648	0.0579	0.2492	0.0900	0.0958	113.0547

According to Figure 5 and Table 6, the results obtained using the linear interpolation model present a convergence in the accuracy as increasing the interpolation samples. Similar behavior is observed in Figure 6 and Table 7, in which the results present a good accuracy from 1296 interpolation samples. Finally, Figure 7 and Table 8 show that the spline interpolation model provides good accuracy from 2401 interpolation samples. It is worth mentioning that the rotor orbits calculated by interpolation models with 256 samples were really far in all simulations.

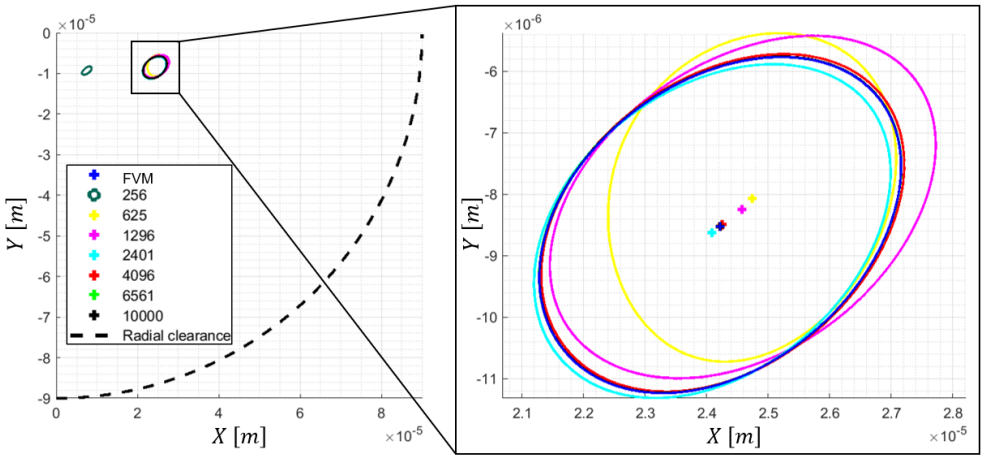

Figure 7. Comparison of rotor orbits in steady-state calculated by spline interpolation.

Table 8. Relative errors of the parameters obtained from rotor orbits calculated by spline interpolation using different numbers of samples.

Interpolation samples database	**Assessment metric**						
	$RE_{e_{o-X}}$[%]	$RE_{e_{o-Y}}$[%]	$RE_{R_{min}}$[%]	$RE_{R_{max}}$[%]	RE_{ψ_o}[%]	MRE_G[%]	T_{sim} [s]
256	69.2919	9.0805	70.6798	57.5925	3.7864	42.0862	135.6191
625	2.1877	5.3370	6.8044	15.1420	41.3261	14.1594	124.2662
1296	1.5004	3.3911	2.8808	5.6744	4.6024	3.6098	131.2193
2401	0.5334	1.1468	1.1358	0.9557	3.4955	1.4534	135.9960
4096	0.1700	0.4327	0.7880	0.3163	0.5153	0.4444	156.7394
6561	0.0084	0.0108	0.0087	0.1849	0.0250	0.0476	163.5495
10000	0.0022	0.0341	0.0922	0.0647	2.4938	0.5374	177.8194

In general, the total time of the simulations showed only small variation. As expected, the surrogate model with lowest computational cost was the linear interpolation, due to its simple procedure, and the one with the highest computational cost was the ANN, due to its higher complexity. However, it is worth mentioning that the total time of simulation using FVM was approximately 1540 seconds.

Comparing with works available in the literature, Sicchieri (2019) proposed a surrogate model to calculate the hydrodynamic forces of journal bearings, based on the Kriging method. The applied Kriging model was trained with 8100 samples and the results also showed a good accuracy. Table 9 presents a comparison of the average time to estimate hydrodynamic forces using the methods proposed in this work and by Sicchieri (2019).

Table 9. Comparison of average time to estimate between different methods.

Method	Finite Volume	Neural Network	Linear Interpolation	Cubic Interpolation	Spline Interpolation	Kriging (Sicchieri, 2019)
Average time [ms]	50.4345	7.4122	0.6699	0.8333	1.1579	7.500

Table 9 shows that surrogate models that need training, i.e. Kriging and Neural Network, have a similar average time. On the other hand, the methods based on interpolations have a lower average time due to be simpler. For all cases, it is possible to note that the average time to perform an estimate of hydrodynamic force with surrogate models is significantly lower when compared to Finite Volume Method.

4. CONCLUSIONS

This work presents a contribution to the modeling of rotating systems supported by journal bearings. For this purpose, the rotor was discretized using the FEM and the hydrodynamic forces of the journal bearings were obtained using different surrogate models, in order to obtain a quick calculation instead the solution of the Reynolds equation by the FVM.

In order to ensure the highest possible accuracy with the smallest database, the application of surrogate models was considered in the analysis of the rotor dynamic behavior assuming different databases sizes. These analyses were carried out based on the response parameters obtained from the rotor orbit in steady state. The surrogate models that showed the best results were cubic interpolations with database from 1296 interpolation samples. Other promising models were spline interpolations with database from 2401 interpolation samples. These models displayed good accuracies obtained from the small databases. However, surrogate models using ANNs showed low accuracy in the results, when compared to the results obtained by interpolation models. The surrogate models that presented the lowest computational cost for the calculation of hydrodynamic forces were linear interpolations, cubic interpolations, spline interpolations and ANNs, in ascending order.

Thus, the results obtained in this paper show that the surrogate models are a promising alternative for a quick calculation of the hydrodynamic forces in journal bearings. In general, surrogate models with more than 1296 interpolation samples provide good accuracy in the results and a low computational cost, when compared to the solution by finite volume method.

5. ACKNOWLEDGEMENTS

The authors would like to thank CAPES, Coordination for the Improvement of Higher Education Personnel for the financial support.

6. REFERENCES

Géron, A., 2019. “Hands-On Machine Learning with Scikit-Learn, Keras, and TensorFlow: Concepts, Tools, and Techniques to Build Intelligent Systems*”. Ed. Sebastopol: O’Reilly*.

Haykin, S. O., 2009. “Neural Networks and Learning Machines”. *Ontario: Pearson Prentice Hall*.

International Standard Organization, 2003. *ISO 1940 – Mechanical vibration - Balance quality requirements for rotors in a constant (rigid) state. Part 1 - Specification and verification of tolerances balance*. Genebra.

Keys, R., 1981. “Cubic convolution interpolation for digital image processing”. *IEEE Transactions On Acoustics, Speech, And Signal Processing*, Vol. 29, No. 6, pp. 1153–1160.

Kornaev, A. V., Kornaev, N. V., Kornaeva, E. P. and Savin, L. A., 2017. “Application of Artificial Neural Networks to Calculation of Oil Film Reaction Forces and Dynamics of Rotors on Journal Bearings”. *International Journal Of Rotating Machinery*, Vol. 2017, p. 1-11.

Lalanne, M. and Ferraris, G., 1990. “Rotordynamics Prediction in Engineering”. *New York: John Wiley and Sons Ltd.*

Lopes, A. and Costa, M., 2018. “Comparison Between Numerical Approximation Methods Using the Matlab Program (in Portuguese)”. *Revista Margens Interdisciplinar*, [S.L.], v. 11, n. 17, p. 14, 25 jan. 2018. Universidade Federal do Para.

Meijering, E., 2002. “A chronology of interpolation- from ancient astronomy to modern signal and image processing”. *Proceedings of the IEEE*, Vol. 90, No. 3, pp. 319–342.

Nelson, H. and Mcvaugh, J., 1976. “The Dynamics of Rotor-Bearing Systems Using Finite Elements”. *ASME Journal of Engineering for Industry*, Vol. 98, No. 2, pp. 593-600.

Pinkus, O. and Lynn, M., 1956. “Analysis of elliptical bearings”. *Trans. ASME*, Vol. 78, No. 16, pp. 965–976.

Ramos, D., 2019. *Effect of cavitation in hydrodynamic bearings on the dynamic behavior of rotors (in Portuguese)*. Master’s Thesis, Graduate Program in Mechanical Engineering, Faculty of Mechanical Engineering, Campinas State University, Campinas, Brazil.

Rosenblatt, F., 1963. “Principles of Neurodynamics: Perceptrons and the Theory of Brain Mechanisms”. *American Journal of Psychology*.

Sacks, J., Schiller, S. B. and Welch, W. J., 1989. “Designs for Computer Experiments”. *Technometrics*, Vol. 31, No. 1, pp. 41-47.

Sicchieri, L. C., 2019. *Kriging metamodeling applied to hydrodynamic bearing models (in Portuguese)*. Master’s Thesis, Graduate Program in Mechanical Engineering, Federal University of Uberlândia, Uberlândia, Brazil.

Simpson, T., Poplinski, J., Koch, P. and Allen, J., 2001. “Metamodels for Computer-based Engineering Design: survey and recommendations”. *Engineering With Computers*, Vol. 17, No. 2, pp. 129-150.

Tuckmantel, F., 2010. Integration of hydrodynamic rotor-bearing systems-support structure for numerical resolution (in Portuguese). Master’s Thesis, Graduate Program in Mechanical Engineering, Faculty of Mechanical Engineering, Campinas State University, Campinas, Brazil.

7. RESPONSIBILITY NOTICE

The authors are the only responsible for the printed material included in this paper.